Analysis of the kinetics of order-parameter fluctuations in the isotropic phase of nematics

L. A. Zubkov, N. V. Orekhova, V. P. Romanov, and S. V. Alimov

A. A. Zhdanov State University, Leningrad
(Submitted 9 July 1986)
Zh. Eksp. Teor. Fiz. **92**, 859–868 (March 1987)

The Maxwell effect and the depolarized light scattering spectrum in the isotropic phase of two liquid crystals are investigated and the temperature dependences of the Maxwell constant and the relaxation time of the order parameter are determined. The spectra are analyzed using an iteration procedure that makes it possible to determine, with the aid of a three-pass Fabry-Perot etalon, relaxation frequencies of the order of several MHz. The change of the temperature of the system as a consequence of heating by a laser beam is investigated. Statistical expressions are obtained for the parameters of the phenomenological theory, and their numerical values are found from an analysis of the experimental data.

It has been established by now that the phenomenological theory of Leontovich[1] and generalizations of this theory[2–4] describe with considerable accuracy the connection that exists in a broad class of liquids between orientational motions and shear deformations. This theory has been subjected repeatedly to experimental verification,[5–9] and has been used successfully to describe, e.g., details of the depolarized light scattering spectrum, and in particular, the fine structure of the wing of the Rayleigh line. Quantitative comparison of the theory with experiment has made it possible to determine the parameters of the phenomenological theory and thereby to establish the fraction of the shear viscosity that is associated with molecular-reorientation processes. Naturally, for different liquids the parameters obtained are slightly different, but the character of the behavior and the temperature dependences in most systems are similar. In recent years the main thrust in the theoretical investigations has been to elucidate the statistical meaning of the parameters of the phenomenological thoery,[10,11] as is necessary for constructing a consistent microscopic theory of orientational relaxation in condensed media.

Nematic liquid crystals (NLC) in the isotropic phase are similar in many respects to ordinary liquids, but fluctuations of the tensor order parameter describing the reorientation increase in a critical manner as the point of the phase transition from the isotropic liquid to the nematic liquid crystal (the *I–N* transition) is approached. This leads to a sharp increase of the scattered-light intensity, to an anomalous increase of the Maxwell constant, and to critical slowing down of the orientational-relaxation time.

A generalization of the Leontovich theory to the case of liquid crystals was carried out by de Gennes.[12] In this theory, as for ordinary liquids, it was assumed that only part of the shear viscosity is associated with the reorientational process, but, in addition, the critical behavior of the fluctuations of the order parameter was taken into account. The theory of de Gennes made it possible to explain the experimentally observed anomalies, but a direct quantitative comparison of the theory with experiment was not performed. This is due to the fact that for such an analysis it is necessary to employ data from different experiments for the same liquid crystal. In ordinary liquids, and also far from the *I-N* transition point,[9] the problem is simplified, since in the depolarized scattering spectrum there is fine structure that determines that part of the shear viscosity which is associated with the reorientational processes. In liquid crystals in the vicinity of the transition point such sharply pronounced features are not observed in the spectrum, and so more experiments are required. On the other hand, this is the only region in which fluctuations of the anisotropy parameter behave in a critical manner and can influence the values and temperature dependence of the coefficients of the phenomenological theory.

In this work, for two liquid crystals, we have carried out a set of measurements necessary to make a complete quantitative comparison with the phenomenological theory. Statistical expressions for the parameters of the de Gennes model are obtained, and their dependence on the temperature is investigated. For a liquid crystal in which the scattering is observed at a wavelength near the intrinsic-absorption edge, we have investigated the change of the temperature in a volume illuminated by a laser beam and in the immediate vicinity of this volume.

1. THE MAXWELL EFFECT AND DEPOLARIZED LIGHT SCATTERING SPECTRUM IN AN NLC

The phenomenological equations describing the kinetics of order-parameter fluctuations $Q_{\alpha\beta}$ in the isotropic phase have the form[12]

$$-a\tau Q_{\alpha\beta}=2\mu\dot{u}_{\alpha\beta}+\nu\dot{Q}_{\alpha\beta},\quad \sigma_{\alpha\beta}=2\eta_0\dot{u}_{\alpha\beta}+2\mu\dot{Q}_{\alpha\beta}; \tag{1}$$

here $a\tau$ is the coefficient of the quadratic term in the expansion of the thermodynamic potential in powers of the order parameter, $\tau=(T-T^*)/T^*$, where T^* is a temperature that is usually 1–2° below the temperature T_c of the first-order *I-N* phase transition, μ and ν are phenomenological coefficients with the dimensions of viscosity, $\sigma_{\alpha\beta}$ is the stress tensor,

$$\dot{u}_{\alpha\beta}={}^1/_2(\partial v_\alpha/\partial x_\beta+\partial v_\beta/\partial x_\alpha),$$

v is the velocity vector, and η_0 is the shear-viscosity coefficient at zero frequency. For the order parameter, as in Ref. 13, we take the traceless part $\varepsilon_{\alpha\beta}$ of the permittivity tensor at an optical frequency.

If a time-independent velocity gradient $\partial v_x/\partial z$ is created in the system, corresponding to the experimental setup for the study of birefringence in flow, we obtain from Eqs. (1)

 0038-5646/87/030484-06$04.00

$$-a\tau\Delta\varepsilon_{zx}=\mu\,\partial v_x/\partial z.$$

Going over from $\Delta\varepsilon_{zx}$ to the difference $n_{\parallel}-n_{\perp}$ of the refractive indices along and perpendicular to the optic axis, we have

$$n_{\parallel}-n_{\perp}=-\frac{\mu}{a\tau n}\frac{\partial v_x}{\partial z}, \tag{2}$$

where n is the refractive index of the unperturbed medium.

It follows from Eqs. (1) and (2) that the orientational-relaxation time τ_f and the Maxwell constant M have the form

$$\tau_f=\nu/a\tau, \quad M=\mu/a\tau n. \tag{3}$$

It is necessary to stress that the numerical value of the coefficient a depends on the choice of order parameter, and in the present work we use the value of a obtained in Ref. 13 for $Q_{\alpha\beta}=\delta\varepsilon_{\alpha\beta}$.

The spectrum of the scattered light of different polarizations has been calculated, e.g., in Ref. 6. Since in NLC the time τ_f is associated with the process of the disordering of regions whose size is of the order of the correlation length, it should be considerably greater than all the other anisotropy-relaxation times. In this case the intensity of the scattered light has the form

$$J_{II}^{V}(\omega)=J_0\left\{\left(\omega^2+\eta_\infty\eta_0\frac{q^4}{\rho^2}\right)\left[\left(\omega^2-\frac{\eta_0 q^2}{\rho\tau_f}\right)^2+\omega^2\left(\frac{1}{\tau_f}+\frac{\eta_\infty q^2}{\rho}\right)^2\right]^{-1}\cos^2\frac{\theta}{2}+\left(\omega^2+\frac{1}{\tau_f^2}\right)^{-1}\sin^2\frac{\theta}{2}\right\}, \tag{4}$$

where θ is the scattering angle, $q=2k\sin(\theta/2)$ is the wave number of the scattering fluctuation mode, $k=2\pi n/\lambda$, λ is the wavelength of the light, and $\eta_\infty=\eta_0-2\mu^2/\nu$ is the nonrelaxing part of the shear viscosity.

We studied the Maxwell effect for two liquid crystals (MBBA and BMOAB) as a function of the temperature. For the measurements we used apparatus consisting of two coaxial cylinders with a gap of width 0.015 cm. The internal cylinder, whose diameter was 4.8 cm and height was 1 cm, served as the roton. The velocity gradient varied in magnitude from 22 to 500 $\sec^{-1}$. The refractive-index difference Δn arising in the liquid flow was measured by a compensation method at wavelength $\lambda=6328$ Å. The dispersion of Δn was negligibly small. The accuracy of the measurements was better than 3%. The results of the measurements were approximated by the formula

$$M=\frac{A}{T-T^*}\exp\left(\frac{T_M}{T}\right). \tag{5}$$

The values of the parameters are given in the caption to Figs. 5a, b.

The relaxation times τ_f of the order parameter are determined from the depolarized light scattering spectrum. The characteristic frequencies $\nu_f=(2\pi\tau_f)^{-1}$ lie in the range 10^6–10^8 Hz. To determine them an instrument with a resolving power of 10^8–10^6 is necessary. This is at the limits of the resolving power for Fabry-Perot interferometers, and, as yet, is not accessible for optical-shift spectroscopy.

We used apparatus in which the spectral instrument was a three-pass Fabry-Perot interferometer with base 12 cm. The scheme of the apparatus is given in Fig. 1. The light source was a single-frequency laser with wavelength $\lambda=5145$ Å. The scattering angle $\theta=90°$. The spectra $I_H^V(\omega)$ of the scattered light was detected by a photomultiplier (PM) with subsequent storage. In the time of a single scan ($\sim$4 sec) the spectrum $I_H^V(\omega)$ of the scattered light was registered in the memory of a multichannel analyzer, as was the spectrum $I_a(\omega)$ of the scattered light from a model system—a latex solution; in the analysis, the latter spectrum was used as the spectrum of the instrumental function of the apparatus. For this, by means of a relay, the laser beam was directed alternately into the thermostat with the liquid crystal and into the cell with the latex, with the latex situated at the same optical distance from the interferometer. The main difficulty in the performance of this experiment was the instability of the laser-radiation frequency. Therefore, we stored only those spectra for which the frequency shift was smaller than 3 MHz. For this, on the display screen of the multichannel analyzer we placed special markers m (Fig. 2a) on both sides of the zero frequencies of the spectra $I_H^V(\omega)$ and $I_a(\omega)$ in the region in which their intensities were varying most sharply. Between 30 and 50 spectra were summed. Typical spectra $I_H^V(\omega)$ and $I_a(\omega)$ are given in Fig. 2. Since, in the entire measured range of temperatures for both crystals, the half-width of the $I_H^V(\omega)$ contour differs little from that of the spectrum of the instrumental function, the usual method of determining the relaxation time from a comparison of their widths is not applicable here.

We have developed a method[14] analogous to that in Ref. 15 and based on the fact that the instrumental function of a

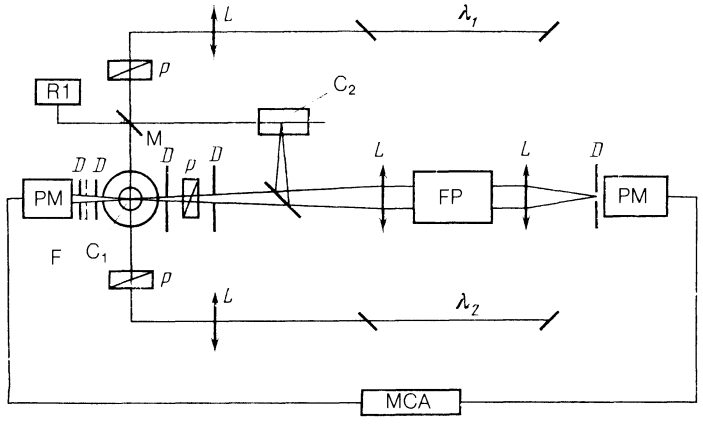

FIG. 1. Scheme of the apparatus for studying the light scattering: λ_1 and λ_2 are the lasers, L are lenses, P are polarizers, D are diaphragms, M is a mirror, R1 is belay, C_1 is a cell with a thermostat, C_2 is a cell with latex, FP is a Fabry-Perot interferometer, MCA is a multichannel analyzer, F is an interference filter, and PM is a photomultiplier.

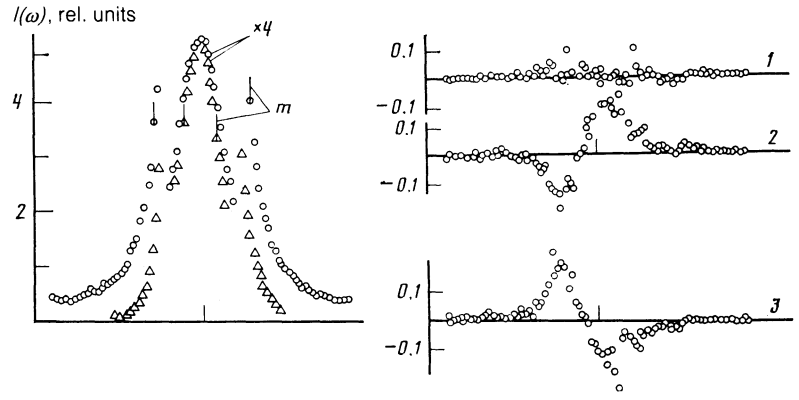

FIG. 2. Experimental spectra: O is the component $I_H^V(\omega)$ recorded in BMOAB at a temperature of 85.4 °C, Δ is the instrumental function $I_a(\omega)$, and m are markers, b) Difference of the experimental and calculated spectra $I_H^V(\omega)$ for different values of the parameter Γ expressed in channels: one channel equals 7.5 MHz. The values of Γ, ν_f, and the residual sum $S(\nu_f,\Gamma)$ are 1) $\Gamma = 0.2$, $\nu_f = 11.8$ MHz, $S(\nu_f,\Gamma) = 34.0$; 2) $\Gamma = 0.7$, $\nu_f = 11.6$ MHz, $S(\nu_f,\Gamma) = 150.0$; 3) $\Gamma = -0.3$, $\nu_f = 12.0$ MHz, $S(\nu_f,\Gamma) = 153.0$.

three-pass Fabry-Perot etalon decreases sharply with frequency, approximately as $(\omega^2+\omega_a^2)^{-3}$ (ω_a is the characteristic frequency of the instrumental function). The spectrum $I_H^V(\omega)$ is the convolution of $I_a(\omega)$ with the spectrum of the physical signal, which in our case is described by Eq. (4):

$$I_H{}^V(\omega) = \sum_{i=-\infty}^{\infty} I_a(\omega-\omega_i+\Gamma) J_H{}^V(\omega_i), \qquad (6)$$

where Γ is the parameter defining the shift that is present between the sets of data for $I_H^V(\omega)$ and $I_a(\omega)$ on account of the discreteness of the multichannel analyzer. It is not difficult to see that the spectrum $I_H^V(\omega)$ differs from the spectrum $I_a(\omega)$, and, in particular, decreases like ω^{-2}, not ω^{-6}, at high frequencies.

The frequency $\omega_f = \tau_f^{-1}$ was determined by the method of least squares from formula (6) with the use of (4). This expression contains four parameters (the amplitude I_0, Γ, η_∞, and ω_f), the latter three parameters appearing nonlinearly. The static viscosity η_0 was measured as a function of the temperature by standard methods. By means of Eq. (3) the quantity η_∞ was represented in the form

$$\eta_\infty = \eta_0 - 2M^2 a\tau n^2 \omega_f, \qquad (7)$$

where the values $a = 32$ J/cm^3 for MBBA and $a = 39$ J/cm^3 for BMOAB were taken from Ref. 13. Thus, the number of unknown parameters was reduced to three: I_0, Γ, and ω_f. The following iteration procedure was used. With a fixed Γ we specified three arbitrary values $\omega_f^{(i)}$. For these values we calculated the residual sum $S(\omega_f^{(i)})$, and through the three points drew the parabola $S(\omega_f)$. The apex of the parabola served to determine ω_f^0. In the subsequent iterations increments $\pm\delta$ were added to the vertex ω_f^0, the residual sums were calculated at these points, the apex of the new parabola was determined, and so on. The procedure was then repeated with a new value of Γ. As the true value of ω_f we took the $\omega_f(\Gamma)$ corresponding to the smallest residual sum.

The effectiveness of the use of multipass interferometers for solving problems of this kind is illustrated in Fig. 3. Here we give the relative error in the determination of ω_f as a function of the ratio ω_f/ω_a for a single-pass and a three-pass interferometer; the curves are obtained by numerical modeling, with spectral-intensity measurements of equal accuracy. For the spectrum $J_H^V(\omega)$ we used a Lorentzian contour.

The degree of coincidence of the calculated spectra with the experimental spectra is shown in Fig. 2b. With allowance for the experimental error, 3–4 iterations were usually required. From the parameter values given in Fig. 2 it can be seen that the value of the residual sum is more sensitive to the value of Γ than to the value of ω_f. This circumstance can turn out to be useful in the determination of the location of lines in the spectrum.

At the exciting-light wavelength $\lambda = 5145$ Å there is appreciable absorption in the BMOAB crysal. It was measured and found to be equal to $\alpha = (2 \pm 0.1)$ cm^{-1}. At the laser powers used (of the order of 5–10 mW) the results of the measurements of ω_f can be distorted as a result of heating of the NLC in the illuminated region. To determine the extent of the heating we measured the integral light-scattering intensity I_H^V, since it is sensitive to change of the temperature and the accuracy of such experiments is sufficiently high (~1%).

The following experiment was set up. The cell with the NLC was illuminated by two lasers—an argon laser with $\lambda_1 = 5145$ Å and a helium-neon laser with $\lambda_2 = 6328$ Å (see Fig. 1). By careful alignment complete coincidence of the two beams in the cell was achieved. An interference filter, making it possible to detect scattering at wavelength λ_2, was placed in the path of the scattered light. The absorption coefficient at λ_2 was of the order of 0.1 cm^{-1}. The intensity of the scattered light was measured in the presence and absence of the radiation with wavelength λ_1. Figure 4 shows the time dependence of I_H^V before and after the argon laser is switched on. It can be seen that the decrease of the intensity

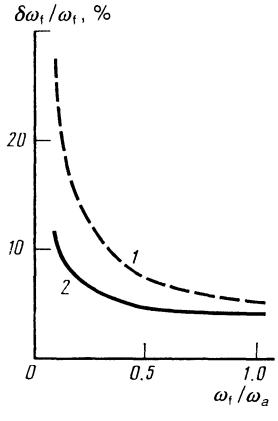

FIG. 3. Calculated dependence of the measurement error $\delta\omega_f/\omega_f$ as functions of the ratio ω_f/ω_a for 1) a single-pass etalon, 2) a three-pass etalon.

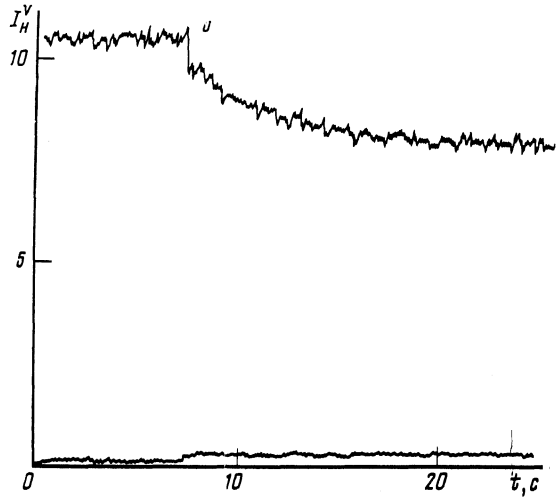

FIG. 4. Time dependence of the scattered-light intensity in BMOAB at $\lambda_2 = 6328$ Å when an argon laser with $\lambda_1 = 5145$ Å is switched on; t_0 is the time at which the laser is switched on, and the lower curve is the contribution of λ_1 to the scattering as a result of luminescence.

I_H^V reaches 25% and has a characteristic time of 1–2 sec. Since in the isotropic phase of the NLC the scattered-light intensity in the first approximation is proportional to $(T - T^*)^{-1}$ (in our experiment, $T - T^* = 2.4°$ before the laser with λ_1 was switched on), this corresponds to a temperature rise of approximately 1 °C in the illuminated volume.

In addition, we made direct measurements of the heating by means of a miniature MT-54 thermoresistor near the beam. The result of the measurements was compared with the result calculated from the heat-conduction equation

$$\frac{\partial^2 T}{\partial r^2} + \frac{1}{r}\frac{\partial T}{\partial r} + \frac{\partial^2 T}{\partial z^2} = -\frac{G}{\chi} e^{-\alpha z}\theta(r - r_0), \qquad (8)$$

where z is the direction of propagation of the beam, χ is the thermal diffusivity coefficient (for BMOAB, $\chi = 1.5 \cdot 10^{-3}$ cm^2·sec^{-1}), $Ge^{-\alpha z}\theta(r - r_0)$ is a term describing the source, $G = I\alpha/(\pi r_0^2 \rho C_p)$, $\theta(x)$ is the theta function, I is the radiation intensity at the laser, ρC_p is the heat capacity per unit volume, r is the distance from the beam axis, and r_0 is the radius of the beam. It is assumed here that the energy distribution over the cross section of the beam is constant.

The solution of Eq. (8) gives the temperature values ΔT (measured with respect to the temperature of the medium) at different distances from the beam:

$$\Delta T(z, r) = \frac{Gr_0}{\chi} \int_0^\infty \frac{ds J_0(rs) J_1(r_0 s)}{s^2 - \alpha^2} \left(e^{-\alpha z} - \frac{\alpha}{s} e^{-sz} \right), \qquad (9)$$

where $J_0(x)$ and $J_1(x)$ are Bessel functions.

In solving (8) we used a Hankel transformation and assumed that $\exp(-\alpha L_0) \ll 1$, where L_0 is the length of the cell, i.e., the second wall of the cell was placed at infinity. As the boundary condition we required the absence of heat flow through the boundary.

With a radiation intensity at the entrance to the cell of the order of 10 W/cm^2 ($r_0 = 2 \cdot 10^{-2}$ cm) for $z = 5$ mm and $r \cong 1.5$ mm, the measured temperature change was 0.5–0.7°, consistent with that calculated from Eq. (9): $\Delta T \cong 0.65°$. The characteristic time τ_T of establishment of this temperature was of the order of 10–15 sec, which agrees with the estimate $\tau_T \sim r^2/\chi$. In the analysis of the experimental data for BMOAB we introduced a correction for heating. For MBBA, $\alpha \cong 0.1$ cm^{-1} and the heating was negligible.

It is important to note that the assumption of a Lorentzian line shape for $J_H^V(\omega)$ (4) leads to systematic overestimates of ω_f. In particular, for MBBA this difference increases from 10–15% near the transition point to 30–40% at $T - T^* \sim 30$–40 °C (Refs. 16 and 17). The temperature dependence of τ_f and the Maxwell constant M are given in Fig. 5.

2. ANALYSIS OF THE EXPERIMENTAL DATA

Using the experimental data for τ_f and M, we calculated the coefficients μ and ν from the Eqs. (3). Their values as functions of the temperature are given in Fig.6. The same figure shows the shear-viscosity contribution $\Delta\eta = 2\mu^2/\nu$ associated with the relaxation of the order parameter. It is interesting to note that the quantity $\Delta\eta$ depends only weakly on the temperature, while the characteristic frequency of

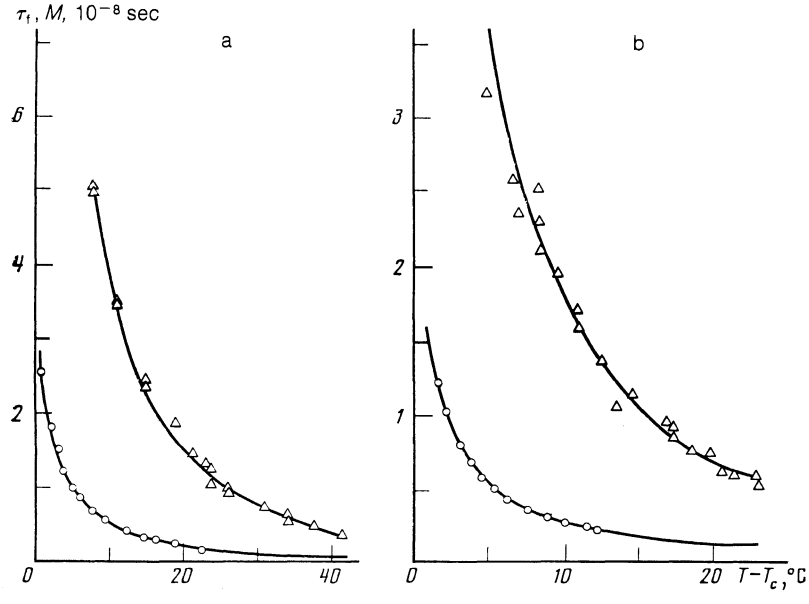

FIG. 5. Temperature dependence of the Maxwell constant M (○) and relaxation time τ_f (△). The solid lines are the approximations $M = A(T - T^*)^{-1} \times \exp(T_M/T)$ and $\tau_f = B(T - T^*)^{-1} \exp(T_f/T)$; a) MBBA: $A = 1.13 \cdot 10^{-11}$ sec·deg, $T_M = 2800$ K, $T^* = 314.7$ K, $B = 4.99 \cdot 10^{-12}$ sec·deg, $T_f = 3750$ K, $T_c = 317.1$ K; b) BMOAB: $A = 1.72 \cdot 10^{-12}$ sec·deg, $T_M = 3000$ K, $T^* = 344.2$ K, $B = 4.06 \cdot 10^{-13}$ sec·deg, $T_f = 4700$ K, $T_c = 345.8$ K.

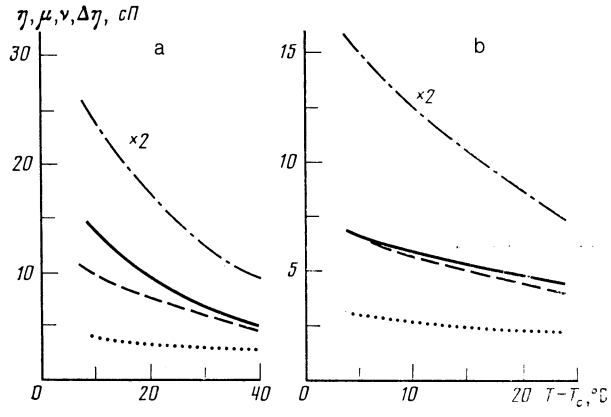

FIG. 6. Temperature dependence of the shear viscosity (the solid line) and the calculated parameters: μ (the dashed line), ν (the dashed-dotted line), $\Delta\eta$ (the dotted line); a) MBBA: $\eta_0 = 0.594\cdot 10^{-6}\exp(4040/T)$ P; b) BMOAB: $\eta_0 = 1.51\cdot 10^{-5}\exp(2954/T)$ P.

this contribution varies in an essentially critical manner. In MBBA $\Delta\eta$ is small and amounts to about 20% of the total shear viscosity. It is probable that this is the reason why in MBBA—the most frequently investigated liquid crystal—shear relaxation has not been detected by direct ultrasonic methods. In Ref. 9 the quantity $\Delta\eta$ for MBBA was determined from the fine structure at temperatures 100–150° higher than T_c and in the analysis of the experimental data it was assumed that the ratio $\Delta\eta/\eta_0$ does not depend on the temperature. From Fig. 6 it can be seen that this assumption is not justified near T_c.

We draw attention to the fact that for both liquid crystals in the entire temperature range investigated the coefficient ν is greater than the total shear viscosity. As follows from Eqs. (1) and (2), the values of both coefficients depend on the choice of the order parameter; therefore, it is not rational to regard these coefficients as viscosities, and only the quantity $2\mu^2/\nu$ has a real physical meaning. It is of interest to attempt to replace μ and ν by parameters that have intuitive physical meaning. For this we shall make use of the statistical method of Mori.[18] According to Ref. 18, for the set of the variables a_j ($j = 1, \ldots, n$) the system of equations describing the variation of a_j in the linear approximation has the form

$$\dot a_j = \langle (iL\hat a_j)\hat a_m\rangle\langle \hat a\hat a\rangle_{ml}^{-1}a_l(t) - \int_0^\infty \langle \hat f_j \hat f_m(-t')\rangle \times \langle \hat a\hat a\rangle_{ml}^{-1}a_l(t-t')\,dt', \quad (10)$$

where L is the Liouville operator, $\hat f_j = (1-\mathscr{P})iL\hat a_j$ is a random force, $\mathscr{P}$ is the projection operator on the set of variables $a_1, \ldots, a_n$, the hats on quantities indicate that they depend explicitly on the coordinates and momenta of the particles of the system, $\langle\ldots\rangle$ denotes averaging over the equilibrium ensemble, and $\langle \hat a\hat a\rangle_{ml}^{-1}$ is an element of the inverse matrix.

If as the variables a_j we choose Fourier components of the momentum and order parameter, we can bring the system (10) to the form

$$\dot Q_{\alpha\beta,\mathbf q} = -\frac{iW}{kT\rho}(q_\alpha P_{\beta,\mathbf q}+q_\beta P_{\alpha,\mathbf q}) - \frac{a\tau}{kT}\xi Q_{\alpha\beta,\mathbf q}, \quad (11)$$

$$\dot P_{\alpha,\mathbf q} = -\frac{\eta_\infty}{\rho}q_\beta(q_\alpha P_{\beta,\mathbf q}+q_\beta P_{\alpha,\mathbf q}) - 2\frac{iWa\tau}{kT}q_\beta Q_{\alpha\beta,\mathbf q}. \quad (12)$$

Here

$$\eta_\infty = \frac{1}{2kTq^2}\int_0^\infty dt\langle \hat f^\perp_{\alpha,\mathbf q}\hat f^\perp_{\alpha,-\mathbf q}(-t)\rangle,$$

where $f^\perp_{\alpha,\mathbf q}$ is the transverse component of the random force conjugate to $P_{\alpha,\mathbf q}$. The coefficients ξ and W are determined by the relations

$$\xi I_{\alpha\beta\gamma\delta} = \int_0^\infty dt\langle \hat f_{\alpha\beta,\mathbf q}\hat f_{\gamma\delta,-\mathbf q}(-t)\rangle, \quad (13)$$

$$WI_{\alpha\beta\gamma\delta} = \langle \hat Q_{\alpha\beta,\mathbf q}\hat Q_{\gamma\delta,-\mathbf q}\rangle, \quad (14)$$

$$I_{\alpha\beta\gamma\delta} = {}^1/_2(\delta_{\alpha\gamma}\delta_{\beta\delta}+\delta_{\alpha\delta}\delta_{\beta\gamma}-{}^2/_3\delta_{\alpha\beta}\delta_{\gamma\delta}),$$

where $\hat f_{\alpha\beta,\mathbf q}$ is the random force conjugate to $\hat Q_{\alpha\beta,\mathbf q}$.

In the derivation of the system (11), (12) it was taken into account that the terms $\langle (iL\hat Q_{\alpha\beta,\mathbf q})\hat Q_{\gamma\delta,-\mathbf q}\rangle$ and $\langle (iL\hat P_{\alpha,\mathbf q})\hat P_{\beta,-\mathbf q}\rangle$ are equal to zero by virtue of the temporal parity of the quantities being averaged, while the quantities $\langle \hat f_{\alpha,\mathbf q}\hat f_{\beta\delta,-\mathbf q}(-t)\rangle$ are set equal to zero in the limit of small $\mathbf q$ by symmetry considerations. The correlator $\langle (iL\hat Q_{\alpha\beta,\mathbf q})\hat P_{\gamma,-\mathbf q}\rangle$ can be rewritten in the form

$$\langle (iL\hat Q_{\alpha\beta,\mathbf q})\hat P_{\gamma,-\mathbf q}\rangle = -\langle \hat Q_{\alpha\beta,\mathbf q}iL\hat P_{\gamma,-\mathbf q}\rangle = iq_\delta\langle \hat Q_{\alpha\beta,\mathbf q}\hat\sigma_{\delta\gamma,-\mathbf q}\rangle.$$

For comparison with the initial equations (1) and (2) it is necessary to make use of the equation of motion

$$\dot P_\alpha = \partial\sigma_{\alpha\beta}/\partial x_\beta \quad (15)$$

and to transform to the spatial Fourier spectrum. Then the system (1), (2) can be rewritten in the following form:

$$\dot Q_{\alpha\beta,\mathbf q} = -i\frac{\mu}{\rho\nu}(q_\alpha P_{\beta,\mathbf q}+q_\beta P_{\alpha,\mathbf q}) - \frac{a\tau}{\nu}Q_{\alpha\beta,\mathbf q}, \quad (16)$$

$$\dot P_{\alpha,\mathbf q} = -\frac{\eta_\infty}{\rho}q_\beta(q_\alpha P_{\beta,\mathbf q}+q_\beta P_{\alpha,\mathbf q}) - i\frac{2\mu a\tau}{\nu}q_\beta Q_{\alpha\beta,\mathbf q}. \quad (17)$$

From a comparison of Eqs. (11), (12) with (16), (17)[1)] it can be seen that in place of the coefficients μ and ν we can introduce the coefficients W and ξ, connected by the simple relations

$$\tau_f = \frac{\nu}{a\tau} = \frac{kT}{a\tau\xi}, \quad M = \frac{\mu}{a\tau n} = \frac{W}{a\tau\xi n}. \quad (18)$$

The quantity ξ (13) is determined by the correlator of the random forces $\hat f_{\alpha\beta,\mathbf q}$, which are the rates of change of the order parameter with the hydrodynamic contribution $\dot Q$ excluded:

$$\xi \sim \int_0^\infty dt\langle \dot{\hat Q}\dot{\hat Q}(-t)\rangle.$$

Consequently, the characteristic length in this correlation function will be not the correlation length but a microscopic length r_0 of the order of the intermolecular distances. From considerations of dimensionality we can conclude that $\xi \sim r_0^3/\tau_0$, where τ_0 has the meaning of the time of reorientation of the individual molecules and should coincide, in order of magnitude, with the orientational-relaxation time obtained from light-scattering spectra in solutions with a low concentration of the NLC. Then it follows from (16) that

$$\tau_f \sim \tau_0 kT/a\tau r_0^3.$$

For example, for MBBA we have $\tau_0 \sim 2\cdot 10^{-10}$ sec (Ref. 17), and for $\tau \sim 5\cdot 10^{-2}$ and $\tau_f \sim 10^{-8}$ sec we obtain $r_0 \sim 6$–8 Å,

i.e., the microscopic length that is characteristic for NLC (Refs. 14, 19, and 20).

The coefficient W determines the correlation of the order-parameter fluctuations with the stress tensor. In the Leontovich theory $W = kT$, while in our case it follows from (18) and (19) that $W \sim (0.3\text{–}0.4)kT$ for both crystals. This, evidently, is connected with the fact that in the NLC, as in other liquids, only part of the stress fluctuations is associated with fluctuations of the orientations, and it is this which leads to the presence of a high-frequency shear viscosity.

In conclusion the authors consider it their pleasant duty to thank L. Ts. Adzhemyan and M. A. Anisimov for discussing the work, and Ya. E. Bolotovskiĭ for help in performing the numerical clculations.

[1)]Equations (12) and (17) pertain to the transverse component of the momentum.

[1]M. A. Leontovich, J. Phys. USSR **4**, 499 (1941).
[2]S. M. Rytov, Zh. Eksp. Teor. Fiz. **58**, 2154 (1970) [Sov. Phys. JETP **31**, 1163 (1970)].
[3]V. P. Romanov and V. A. Solov'ev, Opt. Spektrosk. **29**, 884 (1970) [Opt. Spectrosc. **29**, 470 (1970)].
[4]D. Kivelson and P. A. Madden, Ann. Rev. Phys. Chem. **31**, 523 (1980).
[5]V. S. Starunov, E. V. Tiganov, and I. L. Fabelinskiĭ, Pis'ma Zh. Eksp. Teor. Fiz. **5**, 317 (1967) [JETP Lett. **5**, 260 (1967)].
[6]L. A. Zubkov, N. B. Rozhdestvenskaya, and V. P. Romanov, Zh. Eksp. Teor. Fiz. **65**, 1782 (1973) [Sov. Phys. JETP **38**, 891 (1974)].
[7]C. H. Wang, R.-J. Ma, and Q.-L. Liu, J. Chem. Phys. **80**, 617 (1984).
[8]V. S. Starunov and I. L. Fabelinskiĭ, Zh. Eksp. Teor. Fiz. **66**, 1740 (1974) [Sov. Phys. JETP **39**, 854 (1974)].
[9]G. R. Alms, T. D. Gierke, and G. D. Patterson, J. Chem. Phys. **67**, 5779 (1977).
[10]R. G. Cole, D. K. Hoffman, and G. T. Evans, J. Chem. Phys. **80**, 5365 (1984).
[11]R. A. McPhail and D. Kivelson, J. Chem. Phys. **80**, 2102 (1984).
[12]P. G. de Gennes, *The Physics of Liquid Crystals*, Clarendon Press, Oxford (1974) [Russ. transl., Mir, Moscow (1977)].
[13]L. V. Adzhemyan, L. Ts. Adzhemyan, A. Yu. Val'kov, L. A. Zubkov, I. V. Mel'nik, and V. P. Romanov, Zh. Eksp. Teor. Fiz. **87**, 1244 (1984) [Sov. Phys. JETP **60**, 712 (1984)].
[14]L. V. Adzhemyan, L. Ts. Adzhemyan, L. A. Zubkov, N. V. Orekhova, and V. P. Romanov, Opt. Spektr. **59**, 1169 (1985) [Opt. Spectrosc. **59**, 701 (1985)].
[15]J. Vanderwal, S. M. Mudare, and D. Walton, Opt. Commun. **37**, 33 (1981).
[16]J. D. Litster and T. W. Stinson, J. Appl. Phys. **41**, 996 (1970).
[17]T. D. Gierke and W. H. Flygare, J. Chem. Phys. **61**, 2231 (1974).
[18]H. Mori, Prog. Theor. Phys. **33**, 423 (1965).
[19]E. Gulari and B. Chu, J. Chem. Phys. **62**, 798 (1975).
[20]M. A. Anisimov, M. V. Mamnitskiĭ, and E. L. Sorkin, Inzh.-Fiz. Zh. **39**, 1100 (1980) [J. Eng. Phys. **39**, 1385 (1980)].

Translated by P. J. Shepherd